sciendo

POLISH MARITIME RESEARCH 2 (102) 2019 Vol. 26; pp. 183-197
10.2478/pomr-2019-0038

DESIGN OF JACK-UP PLATFORM FOR 6 MW WIND TURBINE: PARAMETRIC ANALYSIS BASED DIMENSIONING OF PLATFORM LEGS

Paweł Dymarski
Gdańsk University of Technology, Poland

ABSTRACT

The article presents the results of the research conducted within the framework of the project entitled WIND-TU-PLA (ERA-NET, MARTEC II), the general aim of which was to design and analyse supporting structures for wind turbines intended for operation on the South Baltic area. The research part described in the article aimed at developing a preliminary design for a jack-up platform which can operate on water areas with depth of 40 m. The main task was to determine optimal dimensions of platform legs and the radius of their spacing. Two jack-up platform concepts differing by spacing radius and hull dimensions were designed with the intention to be used as a supporting structure for a 6-MW offshore wind turbine. For each concept, the parametric analysis was performed to determine optimal dimensions of platform legs (diameter Dleg and plating thickness tleg). Relevant calculations were performed to assess the movements of the platform with parameters given in Table 1 in conditions simulating the action of the most violent storm in recent 50 years. The obtained results, having the form of amplitudes of selected physical quantities, are shown in comprehensive charts in Fig. 6 and 7. Based on the critical stress values (corresponding to the yield stress), the area was defined in which the impact strength conditions are satisfied (Fig. 14).
Then, the fatigue strength analysis was performed for two selected critical leg nodes (Fig. 12). Its results were used for defining the acceptable area with respect to structure's fatigue (Fig. 14). Geometric parameters were determined which meet the adopted criteria, Table 6. The decisive criterion turned out to be the fatigue strength criterion, while the yield point criterion appeared to be an inactive constraint.

Keywords: support structure, jack-up platform, offshore wind turbine, fatigue, sea loads, parametric study, Morison equation

INTRODUCTION

The history of offshore wind energy utilisation began in 1991, when the first offshore wind farm (Vindeby) was installed in Denmark. Until the end of 2017, the total power output of offshore wind power plants amounted to nearly 19GW [1]. The leading countries in this area are: UK (6836MW), Germany (5355MW), PR China (2788MW), Denmark (1271), Netherlands (1118), and Belgium (877). The contribution of other countries is insignificant.

So far in Poland (year 2018), no offshore wind farms have been built, but significant investors, such as PGE, PKN Orlen, and Polenergia, include building offshore farms in the Polish Exclusive Economic Zone in their development plans. Here, the investment leader is Polenergia, which was the first to obtain the environmental decision for the offshore farm Central Baltic III in July 2016, and then, in April 2017, for the next farm Central Baltic II. The expected total power output of these two farms is 1200MW [2].

At present, offshore wind farms are being built on solid support structures. However, prototypes of floating power plants have also been tested, and in October 2017, a mini floating farm was built which consisted of 5 spar-type platforms – project Hywind [3].

A natural tendency is to build supporting structures which can be installed at increasing depths. Therefore, it is floating structures which attract growing interest of researches and designers. Already, there are designs, and even demonstrators, of semi-submersible platforms [4, 5]. Moreover, the Tension Leg Platform structures have been designed and tested [6, 7, 8]. Numerical analyses have been performed for spar-type platforms [9, 10, 11]

This article presents the results of the research conducted within the framework of the project entitled WIND-TU-PLA, the general aim of which was to design and analyse supporting structures for wind turbines intended for operation on the South Baltic area. The research part described in the article aimed at developing a preliminary design for a jack-up platform which can operate on water areas with depth of about 40 m. The main task was to determine optimal dimensions of platform legs and the radius of their spacing. An assumption was made that the platform rests on three legs. The main criterion was the fatigue strength of the structure on welds. The calculations were performed based on nominal stresses.

Fatigue analyses of supporting structures which utilise plating model-based FEM calculations can be found in [12, 13, 14], while the use of the beam model for analysing the jack-up platform is described in [15].

The jack-up platform belongs to the family of platforms resting on solid base. The platform consists of the deck (platform), a number of legs with feet at their lower ends, and auxiliary devices used for lowering/lifting of legs during installation or change of working area. The concept of the jack-up platform intended to be analysed in this project assumes that the module used for leg lowering/lifting is interchangeable, which makes the production and installation costs of a single platform significantly lower.

The jack-up platform has its own displacement, which allows it to be towed to the destination place. The platform should have positive stability during transportation (when its legs are lifted up).

The advantage of platforms resting on solid structures is their very limited response (movements) to environmental excitations (wind, waves). As a rule, the amplitude of motion of such a platform does not exceed 1 m, even in storm conditions.

Since the platform is supported on three or more legs of very similar length and in similar support conditions, it can be basically assumed that the platform only moves in the horizontal plane, while possible deck rotations about horizontal *Oy*- and *Ox*-axes are very small, and vertical movements are completely negligible.

During the operation, the platform hull (pontoon) stays always over water surface and hydromechanical excitations generated by waves and currents act only on the platform legs. A relatively high position of the platform deck is also favourable with respect to bending moments carried by the turbine tower and the platform as a result of aerodynamic forces acting on the wind turbine.

It was assumed in the project that the jack-up platform can be used on water areas with depth from 30 to 50 m. At greater depths, it seems more profitable economically to use floating platforms, while at smaller depths traditional solutions, such as monopile, jacket, tripod, etc, function sufficiently well [16, 17].

Tripile-type platforms have already been installed at similar depths (up to 50m) (Fig. 1). The advantage of the triple-type platform is its relatively simple structure (platform elements are permanently fixed to each other). However, proper preparation of the foundation is required in this case, and the platform elements can only be installed using special (large) vessel. Moreover, a platform of this type does not have own displacement, nor hydromechanical stability during transportation.

Fig.1. Tripile-type platforms – project BARD offshore 1 – Germany. Approximate depth of water area 40m [www.windpoweroffshore.com,www.hadel.net]

The main problems which had to be solved when designing the preliminary prototype of the jack-up platform included determining the amplitude of motion of the hull and the nacelle, and assessing the internal forces carried by the main structural components (legs, tower, hull) as functions of dimensions of basic platform components. The performed parametric analysis made the basis for determining boundaries of the acceptable area with respect to structural loads. Moreover, parameters were determined which best fulfilled a given target function (stress minimisation, or structure mass minimisation for the assumed acceptable stresses, for instance).

CALCULATION MODEL FOR PARAMETRIC ANALYSIS

For the purpose of the parametric analysis, a simplified model with two degrees of freedom (DOFs) was developed. The first DOF was the linear (horizontal) motion of platform hull, while the second DOF was the linear (horizontal) motion of nacelle with turbine.

The platform hull rests on three legs anchored to the seabed. Each leg ends with a foot of larger diameter, the underside of which has the shape of an inverted cone or pyramid, Fig. 2. The legs are permanently fixed to the hull. The nacelle and the hull are connected together by the tower (single tube) permanently fixed to the hull. It is assumed that the tower column can freely rotate at the nacelle side, due to small moment of inertia of the nacelle with turbine (bending moment equal to zero).

It was assumed at the preliminary stage that the stiffness of the hull is much larger than that of the legs and tower (the hull does not deform). Due to this large hull stiffness and due to the fact that the hull is supported on three legs, the hull rotation about the horizontal axis which is perpendicular to

the wave propagation direction *Oy* does not exist. That means that the rotations of leg ends are blocked at points of their connection with the hull. Similarly, the rotation of the tower at the point of its connection with the hull is also blocked. Another simplifying assumption which was adopted is that the ground under the platform is so flexible that it does not block the leg rotation. Consequently, an articulated joint was assumed at lower end of each leg (which is a conservative approach). The structural scheme of the platform is shown in Fig. 3.

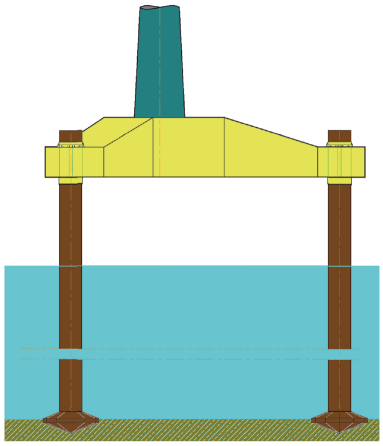

Fig. 2. Scheme of jack-up platform foundation

The stiffness of a single leg with respect to horizontal hull motion is:

$$k_{1leg}=\frac{3\,EI_{leg}}{l_{leg}^3}\quad , \tag{1}$$

Then, the stiffness of the joint between hull and nacelle with respect to relative horizontal hull/nacelle motion is:

$$k_{tower}=\frac{3\,EI_{tower}}{l_{tower}^3}\quad , \tag{2}$$

where:

E is the modulus of elasticity of steel,

I_{leg}, I_{tower} are the moments of inertia of the cross sections of a single leg and the tower, respectively,

l_{leg}, l_{tower} are the length of the legs and the height of the tower (measured from pontoon deck to turbine axis), respectively, see Table 2.

The above formulas were used for creating the structural stiffness matrix in the simplified model.

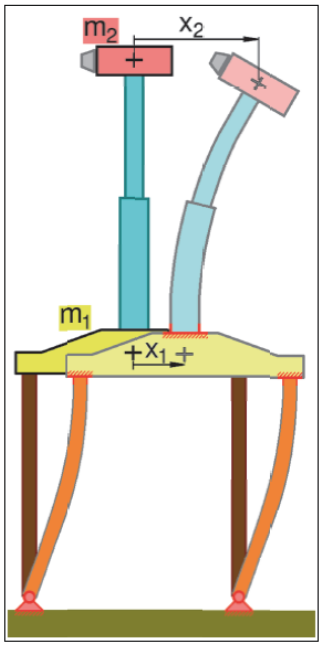

Fig. 3 Structural strength scheme of jack-up platform with tower. Determining degrees of freedom.

STIFFNESS MATRIX. EQUATION OF PLATFORM MOTION

Stiffness matrix

The forces acting on the hull and nacelle as a result of dislocation of main structure nodes are given by the formula [18, 19]:

$$\begin{bmatrix}F_1^{stiff}\\F_2^{stiff}\end{bmatrix}=-\begin{bmatrix}k_{1,1} & k_{1,2}\\k_{2,1} & k_{2,2}\end{bmatrix}\begin{bmatrix}x_1\\x_2\end{bmatrix}, \tag{3}$$

where:

F_1^{stiff}, F_2^{stiff} are the generalised forces resulting from dislocation of relevant structure nodes (1 or 2); $k_{i,j}$ are the stiffness matrix elements which define the force acting at the i-th node due to (elementary) dislocation of the j-th node, and x_1, x_2 are the node dislocations.

Elements of stiffness matrix:

$k_{1,1}$ - describes the force acting at node 1 as a result of elementary node dislocation with respect to the immovable remaining nodes and supports:

$$k_{1,1}=n_{leg}k_{1leg}+k_{tower}\quad , \tag{4}$$

where:

n_{leg} is the number of platform legs.

$k_{1,2}$, $k_{2,1}$ – describe the force acting at node 1 as a result of elementary dislocation of node 2, and the force acting at node 2 as a result of elementary dislocation of node 1:

$$k_{1,2}=k_{2,1}=-k_{tower} \tag{5}$$

$k_{2,2}$ – describes the force acting at node 2 as a result of elementary dislocation of this node:

$$k_{2,2}=k_{tower} \tag{6}$$

The structural model of the platform is linear, but the external excitations acting on the platform and the turbine have the form of aero- and hydrodynamic forces described by the expanded Morison equation [20,7]. The force acting on the *i*-th fragment of the structure (leg segment, for instance) is given by the formula:

$$F_{x,i}=\frac{1}{2}C_{D,x}\rho A_{p,x}|u-\dot{x}|(u-\dot{x})+\rho V_b(1+C_{A,x})\frac{\partial u}{\partial t}-\rho V_b C_{A,x}\ddot{x} \quad , \tag{7}$$

where
$C_{D,x}$ is the drag coefficient in the *x* direction,
ρ is the fluid density,
$A_{p,x}$ is the projection of the segment area onto the *x* direction,
u is the fluid velocity component in the *x* direction,
V_b is the volume of the segment (fragment of structure),
$C_{A,x}$ is the added water mass coefficient in the *x* direction,
$\dot{x}$, $\ddot{x}$ are the segment velocity and acceleration in the *x* direction, respectively.

The main force acting on the nacelle is the turbine thrust force [21], which should be additionally complemented by the aerodynamic drag force acting on the upper part of the tower:

$$F_2=\frac{1}{2}C_T\rho_{air}A_T|u_{w,2}-\dot{x}_2|(u_{w,2}-\dot{x}_2) +\frac{1}{2}C_{D,tower}\rho_{air}A_{p,tower}|u_{w,2}-\dot{x}_2|(u_{w,2}-\dot{x}_2) \quad , \tag{8}$$

where C_T is the turbine thrust coefficient, $C_{D,tower}$ is the tower drag coefficient, ρ_{air} is the air density, A_T is the turbine circle area, $A_{p,tower}$ is the tower projection onto the *x* direction, $\dot{x}_2$ is the velocity of node 2 (nacelle), and $u_{w,2}$ is the wind velocity at the nacelle height.

The forces acting on the platform hull (pontoon) can be described as:

$$F_1=F_{1,hydro}(t)+\frac{1}{2}C_{D,hull}\rho_{air}A_{p,hull}|u_{w,1}-\dot{x}_1|(u_{w,1}-\dot{x}_1) \quad . \tag{9}$$

The first term on the right-hand side of Equation 9 represents the hydrodynamic forces (this issue will be discussed further in the article), while the second term represents the aerodynamic thrust force acting on the hull. $C_{D,\mathrm{hull}}$ is the hull (pontoon) drag coefficient, $A_{p,hull}$ is the projection of the hull surface area onto the *x* direction, $\dot{x}_1$ is the velocity of node 1 (hull), and $u_{w,1}$ is the wind velocity at the hull height.

The forces acting directly on the platform (hull) are relatively small. The main external excitation being the source of platform motion is the excitation acting on platform legs. The elementary force acting on the leg segment of length δ*z* is [20]:

$$\delta F_{sect}=\frac{1}{2}C_D\rho A_{p,sect}|u-\dot{x}_{sect}|(u-\dot{x}_{sect}) +\rho V_{b,sect}(1+C_A)\frac{\partial u}{\partial t}-\rho V_{b,sect}C_A\ddot{x}_{sect} \quad , \tag{10}$$

where: C_D, C_A are the drag coefficient and the added mass coefficient of legs (see table 2), ρ is the water density, $A_{p,sect}$ is the projection of the surface area of the structure segment onto the x direction, $V_{b,sect}$ is the (submerged) volume of the structure segment, *u* is the water velocity, and , $\dot{x}_{sect}$, $\ddot{x}_{sect}$ are the velocity and acceleration of the structure segment, respectively.

Let us consider the platform leg as a beam resting on two supports: seabed at the bottom (simple support), and platform at the top (blocked rotation). If the force F_{sect} acts on the leg segment, then the leg acts on the platform with the force equal to the reactive force at the support [22]:

$$\delta F_{1,hydro}=\delta F_{sec}\left[1-\frac{a^2}{2l_{leg}^3}(3l_{leg}-a)\right], \tag{11}$$

where $a = z_{hull} - z_{sect}$ is the distance between the segment of concern and the point of leg-hull fixing.

Finally, the total hydromechanical force passed from the legs to the platform is:

$$F_{1,hydro}(t)=\sum_{i_{leg}}\int_{-d}^{0}q(z,t)\left[1-\frac{(z_{hull}-z)^2}{2l_{leg}^3}(3l_{leg}-(z_{hull}-z))\right]dz \tag{12}$$

The continuous load *q(z)* acting on platform legs can be determined from Equation 13:

$$q(z,t)=\frac{1}{2}C_D\rho D_{leg}|u-\dot{x}|(u-\dot{x}) +\rho\frac{\pi D_{leg}^2}{4}(1+C_A)\frac{\partial u}{\partial t}-\rho\frac{\pi D_{leg}^2}{4}C_A\ddot{x} \tag{13}$$

The water velocity *u=u(x,z,t)* is calculated based on the theory of waves (the Airy model, or the second-order Stokes model [18, 19, 20, 23, 24]). The position *x=x(z,t)* of a given leg section and its derivatives (velocity and acceleration) are given by the hull position x_1 and the modal function of leg deflection, which can be approximately defined (based on support conditions) as:

$$x(z,t)=x_1(t)\psi(z)$$

where

$$\psi(z)=\sin\left[\frac{\pi(z-z_{base})}{2l_{leg}}\right] \tag{14}$$

The last term in Equation 13 represents the force acting on the legs during the accelerated motion, and is related with the presence of the added mass. The acceleration of a selected leg section can be determined via double differentiation of Equation 14

$$\ddot{x}(z,t)=\ddot{x}_1\psi(z) \tag{15}$$

If we define the last term in Equation 9 as $q_{am}(z,t)$, i.e.:

$$q_{am}(z,t)=-\rho\frac{\pi D_{leg}^2}{4}C_A\ddot{x} \tag{16}$$

then the force passed to the platform can be obtained from Equation 8 as:

$$F_{1,am}(t)=-m_a\ddot{x}_1 \tag{17}$$

where the added mass m_a is calculated from formula:

$$m_a=\rho\frac{\pi D_{leg}^2}{4}C_A\sum_{i_{leg}}\int_{-d}^{0}\psi(z)\left[1-\frac{(z_{hull}-z)^2}{2l_{leg}^3}\left(3l_{leg}-(z_{hull}-z)\right)\right]dz, \tag{18}$$

or:

$$m_a=n_{leg}\rho\frac{\pi D_{leg}^2}{4}d\cdot C_A f_{1,am},$$

where:

$$f_{1,am}=\frac{1}{d}\int_{-d}^{0}\psi(z)\left[1-\frac{(z_{hull}-z)^2}{2l_{leg}^3}\left(3l_{leg}-(z_{hull}-z)\right)\right]dz \tag{19}$$

The coefficient $f_{1,am}$ represents part of the added mass which contributes to the increase of the force of inertia at a given node of the structure (here: platform hull) as a result of the motion of this node. The above coefficient ranges from 0 to 1. The diagram of its changes as a function of relative leg draught d/l_{leg} for boundary conditions as in the discussed issue is shown in Fig. 4

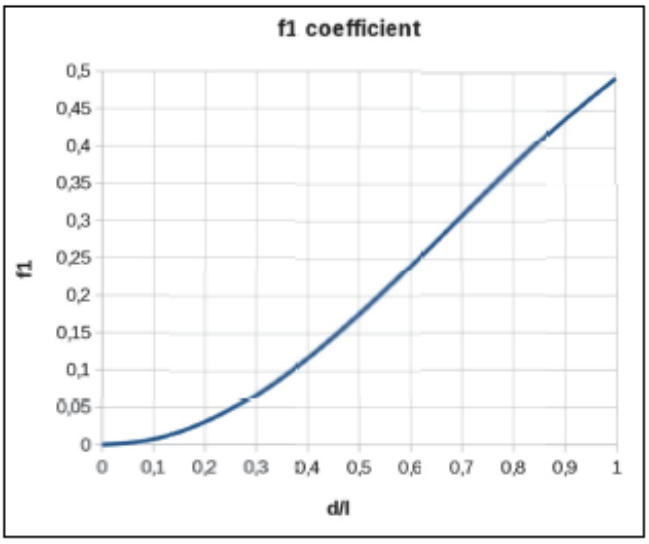

Fig. 4. Coefficient f_1 describing the contribution of leg related added water mass to platform hull inertia as function of relative leg draught d/l_{leg}

Equation of platform motion

The equation of motion of the platform as an object with two degrees of freedom has the following form:

$$\begin{bmatrix}m_1 & 0\\ 0 & m_2\end{bmatrix}\begin{bmatrix}\ddot{x}_1\\ \ddot{x}_2\end{bmatrix}+\begin{bmatrix}k_{1,1} & k_{1,2}\\ k_{2,1} & k_{2,2}\end{bmatrix}\begin{bmatrix}x_1\\ x_2\end{bmatrix}=\begin{bmatrix}F_1(x_1,\dot{x}_1,\ddot{x}_1,u)\\ F_2(x_2,\dot{x}_2,\ddot{x}_2,u_{w,2})\end{bmatrix} \tag{20}$$

where m_1, m_2 are the masses of relevant nodes of the structure (hull, nacelle, see Fig. 3) with part of the mass of the elements connecting these nodes (legs, tower).

Although this equation does not include explicitly a damping term, damping is present in the right-hand side of the excitation vector $[F_1\ F_2]^T$. Due to nonlinear nature of damping, it cannot be explicitly "extracted".

DESCRIPTION OF SELECTED HYDRO-METEOROLOGICAL CONDITIONS

It was assumed in the model that the platform can be subjected to the action of wind, waves and sea currents. The effect of sea currents on platform dynamics is relatively small, and usually has the form of intensified damping of platform motion. It was assumed in the calculations that for the wind velocity $u_{w,2}$=25m/s, which is the value similar to those recorded in violent storms, the surface water velocity is $u_{curr}(0)$=0.45 m/s. It was also assumed that the vertical velocity distribution profile below sea surface is exponential (Equation 21) [18]. This distribution profile was confirmed in measurements performed at the Maritime Institute in Gdansk [23].

$$u_{curr}(z)=\left(1+\frac{z}{d}\right)^{1/7}\cdot u_{curr}(0) \tag{21}$$

The analysis was performed using weather conditions corresponding to the most violent storm in recent 50 years. The following wave conditions were assumed as a result of statistical data processing at the Maritime Institute in Gdansk [23]:

Significant wave height: H_s=9.01m, peak period: T_p=11.3s, peak shape coefficient: γ=4.14.

The waves were modelled using the JONSWAP spectrum [24].

The method to determine the velocity and acceleration of fluid particles based on the assumed wave spectrum can be found in [24, 16, 23].

The analyses were performed for the 50-years' storm with time duration of 3600 seconds. Prior to that, the analysis of results had been performed for three variants of waves in such a storm, which differed by random parameters. Then, one variant was selected in which the highest wave was recorded, along with the highest amplitude of structural response.

For the above wave parameters, the obtained significant amplitude of the horizontal water velocity component is $u_{A,1/3,z=0}$ =2.8 m/s at surface and $u_{A,1/3,z=-40m}$ =1.3 m/s near the seabed. Taking additionally into account the range of leg diameter changes (Table 1), we arrive at the range of the Keulegan-Carpenter number K_C=4-11. The maximal (and also dominating) value of the added water mass coefficient

within this range of K_C is: C_A=1.0 [25, 23]. The assumed drag coefficient is C_D=1.0, which is the smallest value in the above range of K_C (conservative approach).

The calculations were performed for the following wind velocities at turbine axis height:
$u_{w,2}$=25m/s, $u_{w,2}$=11.4m/s and $u_{w,2}$=0m/s

The velocity $u_{w,2}$=25m/s is the velocity of turbine shut-down, while $u_{w,2}$=11.4m/s is the velocity of maximal turbine thrust, and $u_{w,2}$=0m/s represents the zero (average) thrust. This last velocity corresponds to minimal real thrust and the resulting minimal aerodynamic damping, which is why this state can generate relatively high amplitudes.

The results obtained for $u_{w,2}$=25m/s are less favourable than those for $u_{w,2}$=11.4m/s, as the turbine thrust is significantly smaller [27, 28], with the resulting smaller damping of the motion generated by aerodynamic forces. The least favourable conditions are for $u_{w,2}$=0m/s. However, it was decided that the absence of wind combined with the presence of maximal waves is a highly unlikely variant. For statistical reasons, this case cannot be the subject of the fatigue analysis making use of Weibull distribution.

The results presented further in the article refer to the case $u_{w,2}$=25m/s.

DESCRIPTION OF SELECTED MODEL PARAMETERS AND DETERMINING THEIR RANGES

The main model parameters are those describing the geometry of platform legs: diameter D_{leg} and plating thickness t_{leg}.

The next parameter whose effect on the dynamics of the structure was analysed was the leg spacing radius r_{leg}, i.e. the distance of legs from central platform axis.

The first two parameters are decisive for leg strength characteristics: stiffness EI_{leg} and bending coefficient $W_{leg}=2I_{leg}/D_{leg}$,

The third parameter affects the mass of the hull (length of platform "arms") and the distribution of axial forces in legs, due to the action of the moment generated by the turbine thrust force.

The matrix of parameters for which the calculations were performed is given in Table 1:

Tab.1. Matrix of parameters of jack-up platform

	r_{leg} = 20 m			r_{leg} = 25 m		
	D_{leg}=2.8 m	D_{leg}=3.2 m	D_{leg}=3.6 m	D_{leg}=2.8 m	D_{leg}=3.2 m	D_{leg}=3.6 m
t_{leg}=50 mm	x	x	x	x	x	x
t_{leg}=60 mm	x	x	x	x	x	x
t_{leg}=70 mm	x	x	x	x	x	x

The remaining geometric/mass parameters are collated in Table 2. The hull masses M_{hull} have been approximately determined based on a preliminary draft of the structure, which was used for assessing the hull plating surface area. The assumed average thickness of plating was t_p=20mm.

Tab.2. Main quantities assumed in calculations

Mass of hull "alone" (for r_{leg}=20 m and r_{leg}=25 m)	M_{hull}=520 t, 600 t
Mass of nacelle with turbine	$m_{nacelle}$=480 t
Length of legs, to platform bottom	l_{leg0}=52 m
Length of legs assumed in calculations (including hull height)	l_{leg}=54 m
Height of tower (from deck to turbine axis)	h_{tower}=75 m
Height of turbine axis	h_{turb}=95 m
Tower diameter in lower part (to half length)	$D_{1,tower}$=6.25 m
Tower plating thickness in lower part	$t_{1,tower}$=35 mm
Tower diameter in upper part (to half length)	$D_{2,tower}$=5.5 m
Tower plating thickness in upper part	$t_{2,tower}$=25 mm
Added mass coefficient of legs	C_A=1.0
Drag coefficient of legs	C_D=1.0
Drag coefficient of tower	$C_{D,tower}$=0.8

The turbine data were selected based on the manufacturer's data [26]. However, since the manufacturer does not make all data available (aerodynamic coefficients, for instance), some of the assumed values, turbine thrust coefficient CT, for instance, were taken from the description of the reference turbine of the US National Renewable Energy Laboratory – NREL 5MW [27]. Also, the 6MW DOWEC turbine has similar coefficients [28].

Tab.3. Turbine data for jack-up platform. The data of turbines SENVION and NREL included for comparison.

Type	Senvion 6.2M	NREL 5 MW	**Value assumed for simulations**
Turbine power	6.15MW	5 MW	**6 MW**
Rated wind speed	14.0 m/s	11.4 m/s	**11.4 m/s**
Max working speed of wind	30 m/s	25 m/s	**25 m/s**
Diameter of rotor	126 m	126 m	**126 m**
RPM range	7.7 – 12.1 rpm	6.9 – 12.1 rpm	-
Mass of nacelle+rotor	480 tonnes	350 tonnes	**480 tonnes**
Height of rotor axis	85 m – 117 m	90 m	**95 m**
Thrust coefficient C_T (11.4 m/s, 25 m/s)	N/A	0.73, 0.074	**0.73, 0.074**

RESULTS OF PARAMETRIC ANALYSIS

The results of the parametric analysis are presented in the form of time-histories of the following quantities: position x and acceleration $\ddot{x}$ of nacelle and hull, longitudinal stresses in platform legs $\sigma_{n,leg}$ and in tower plating $\sigma_{n,tower}$, and maximal bending moments in platform legs M_{leg} and in tower M_{tower}.

The diagrams of position, acceleration, stresses and bending moments for the selected set of parameters are shown in Fig. 5 a-d. These diagrams, together with those obtained from calculations for other sets of parameters, have made the basis for preparing bar graphs of extreme values as functions of leg diameter D_{leg} and plating thickness t_{leg} (see Fig. 6-7).

These bar graphs can be used for determining the range of acceptable solutions and selecting a point, or area, which is optimal with respect to the assumed criteria.

Additionally, the diagrams in Figs. 8-9 present the mass of the structure (without nacelle and turbine) as a function of parameters.

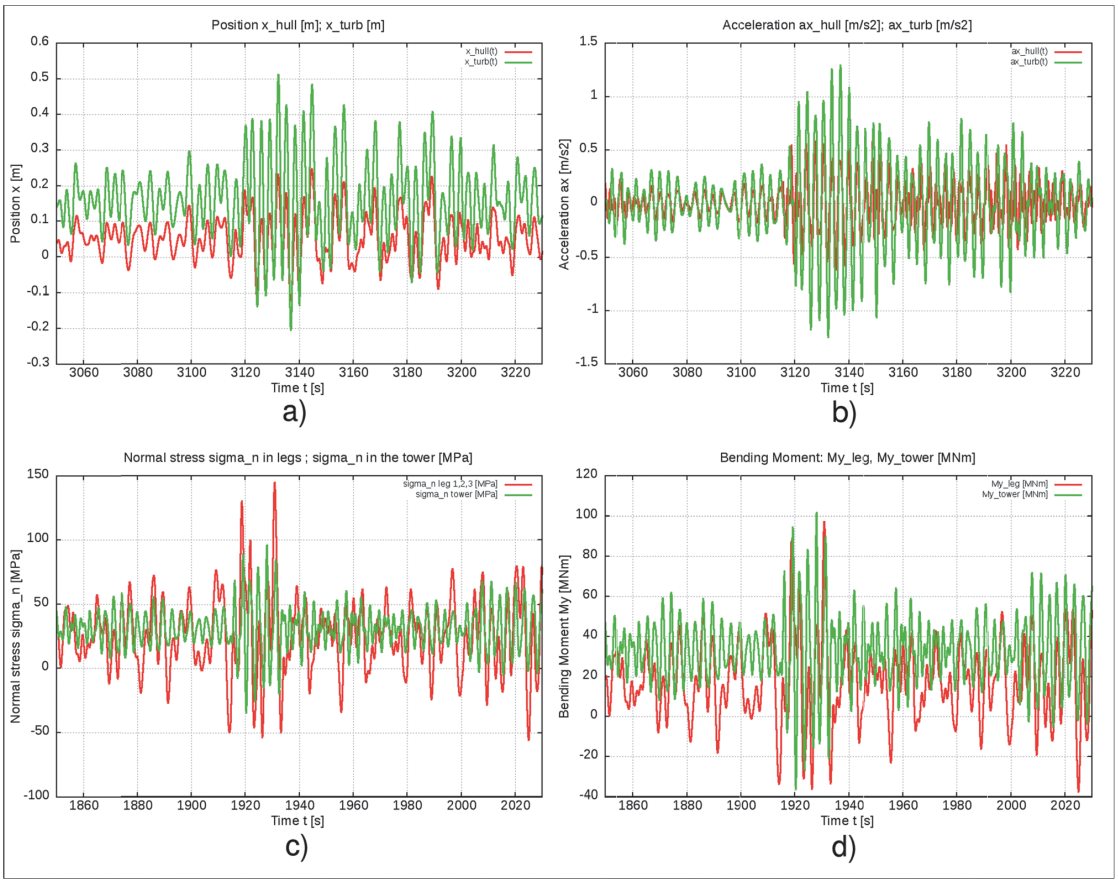

Fig. 5. Platform variant: r_{leg} = 25 m, D_{leg}=3.6 m, t_{leg}=70 mm. Sea conditions: H_s=9.0 m, T_p=11.3 s, γ=4.14, wind speed U_w=25 m/s. Time-histories of: a) longitudinal oscillations of hull and nacelle: $x_{hull} = x_{hull}(t)$, $x_{turb} = x_{turb}(t)$; b) longitudinal accelerations (along x-axis) of hull and nacelle: $a_{x,hull} = a_{x,hull}(t)$, $a_{x,turb} = a_{x,turb}(t)$; c) normal stresses in hull legs $\sigma_{n,leg}$ and in tower plating $\sigma_{n,tower}$; d) maximal bending moments in hull legs $M_{y,leg}$ and in tower plating $M_{y,tower}$.

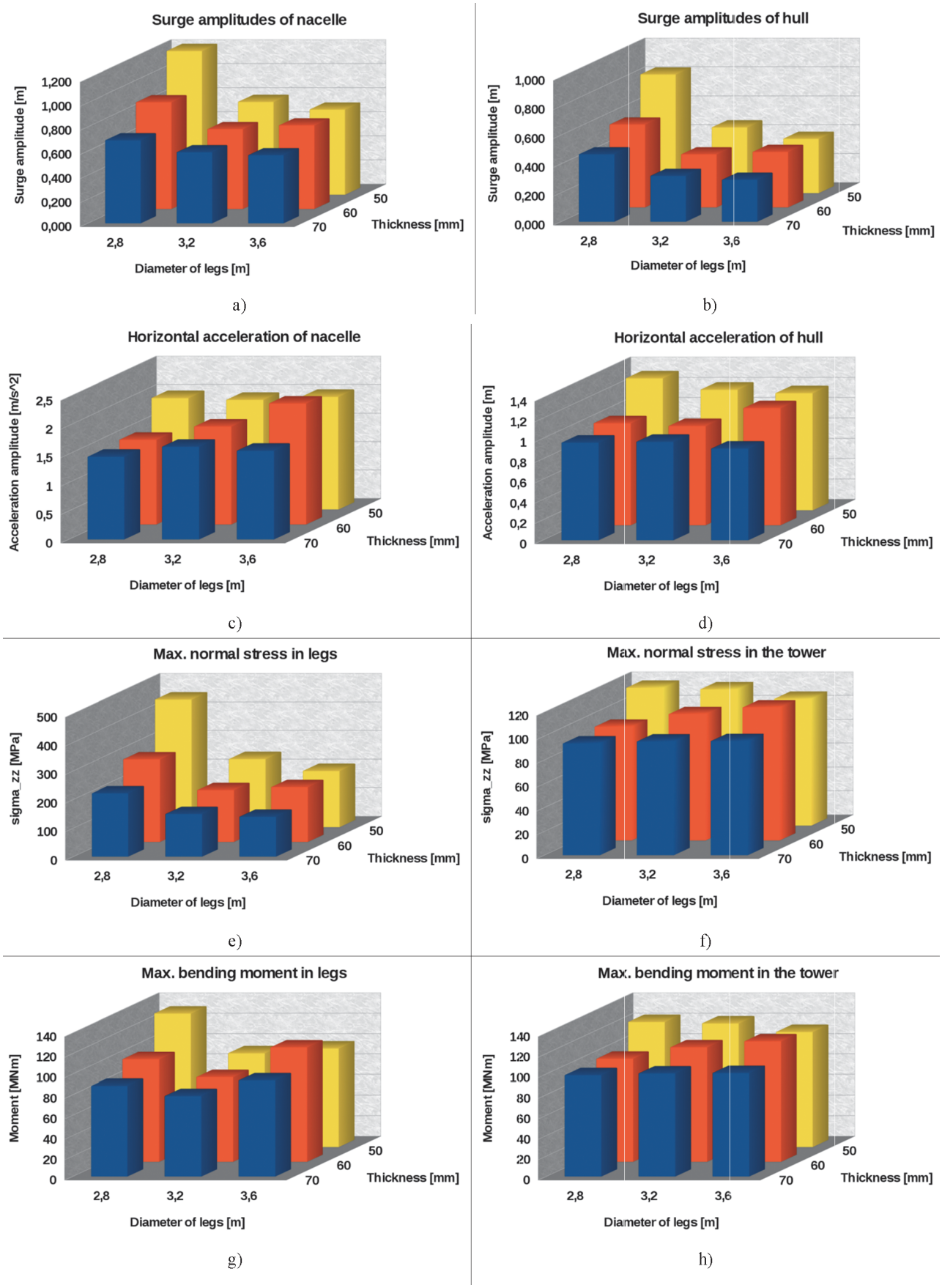

Fig. 6. Jack-up platform, r_{leg}=20m: a-d) Amplitudes of movements and accelerations of nacelle and hull; e), f) maximal stresses in hull legs and in tower plating, g), h) internal forces in hull legs and in tower plating.

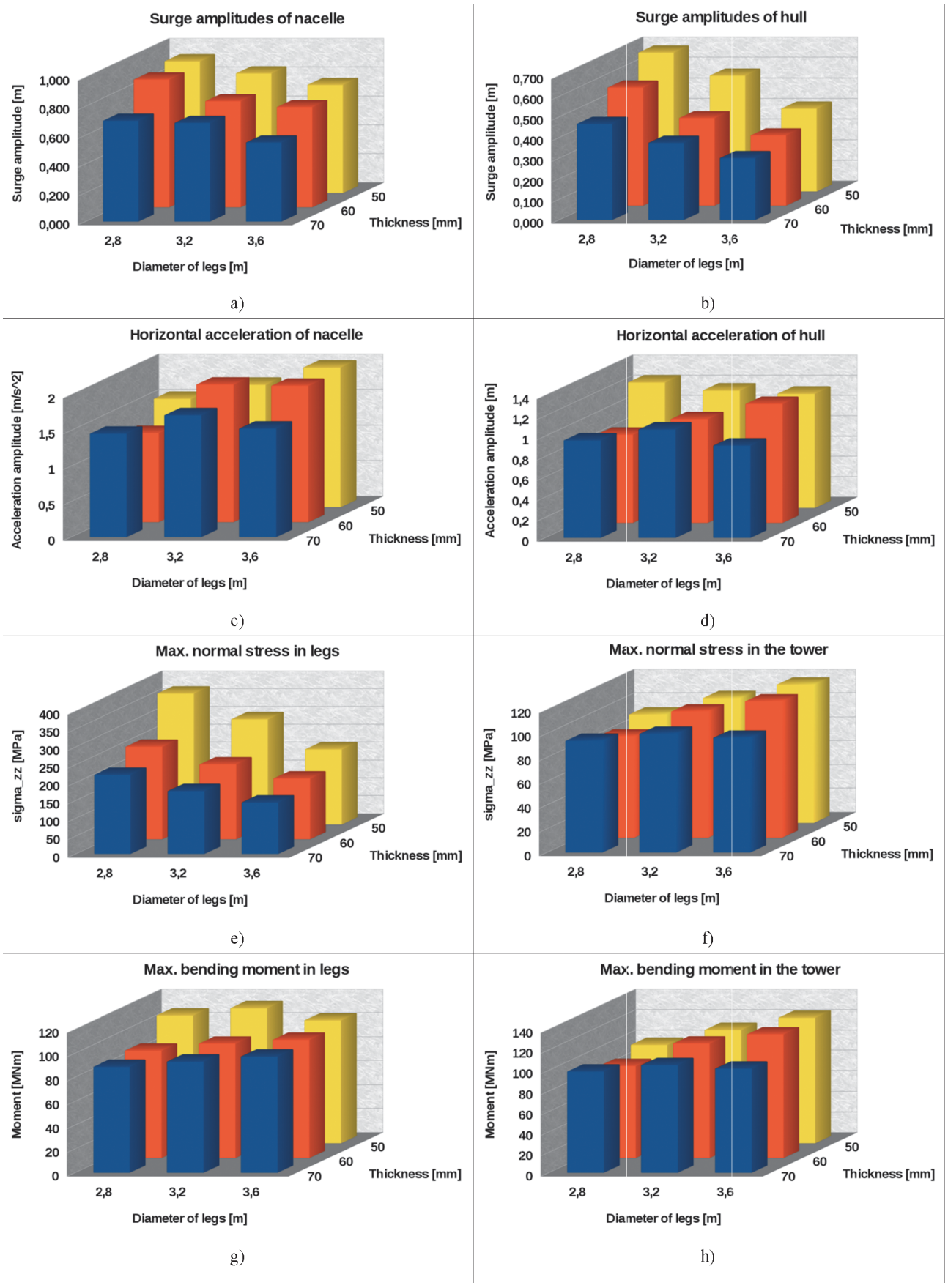

Fig. 7 Jack-up platform, r_{leg}=25m: a-d) Amplitudes of movements and accelerations of nacelle and hull as functions of parameters D_{leg} and t_{leg}; e), f) maximal stresses in hull legs and in tower plating, g), h) internal forces in hull legs and in tower plating.

Additionally, Table 4 collates the masses of the structure as a function of parameters. The mass of steel is a decisive factor for the price of the structure, it also affects the price of its transportation and installation. This way, it is a factor which limits, for economic reasons, the area of applicable solutions.

The mass of the structure increases with the increase of leg diameter and plating thickness. On the other hand, the stresses in platform legs decrease with the increase of leg diameter and/or plating thickness. The mass and stress bar graphs are shown in Fig. 8 and Fig. 9. They reveal that the optimal solution should be searched on the line of acceptable stresses. Determining the acceptable values at selected nodes will be discussed in detail in the next Chapter.

Table 4. Mass matrix of jack-up platform structure as function of parameters. The presented values include the masses of hull, legs, and tower, but exclude the masses of nacelle and turbine.

	r_{leg} = 20 m			r_{leg} = 25 m		
	D_{leg}=2.8 m	D_{leg}=3.2 m	D_{leg}=3.6 m	D_{leg}=2.8 m	D_{leg}=3.2 m	D_{leg}=3.6 m
t_{leg}=50 mm	*1465 t*	*1553 t*	*1641 t*	*1545 t*	*1633 t*	*1721 t*
t_{leg}=60 mm	*1588 t*	*1694 t*	*1800 t*	*1668 t*	*1774 t*	*1880 t*
t_{leg}=70 mm	*1712 t*	*1835 t*	*1959 t*	*1792 t*	*1915 t*	*2039 t*

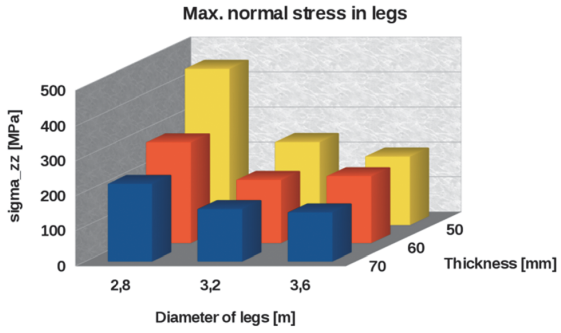

a)

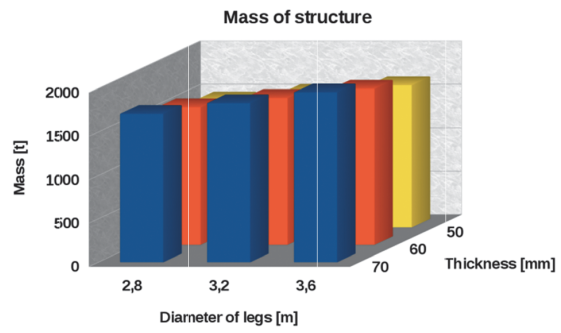

b)

Fig. 8. Bar graphs of maximal stresses in legs (a) and platform mass (b) as functions of parameters D_{leg} and t_{leg} for platform leg spacing radius r_{leg} = 20 m.

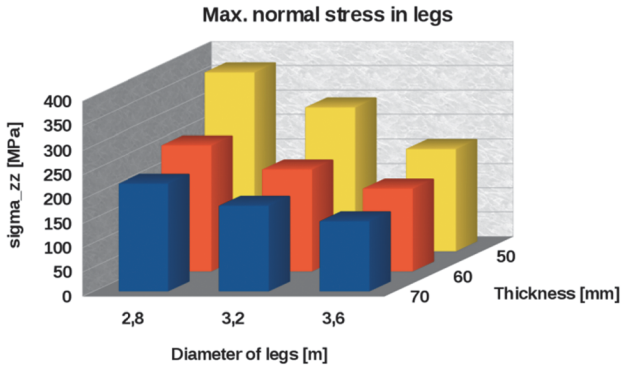

a)

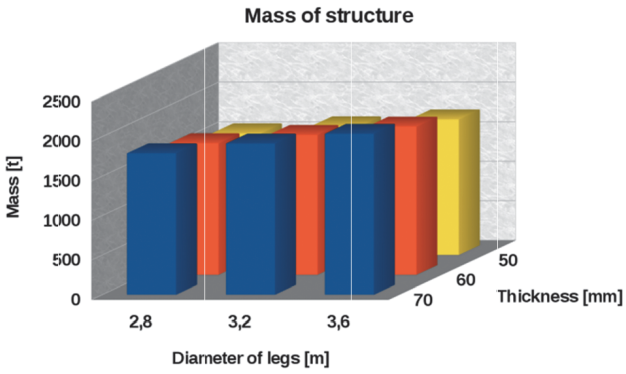

b)

Fig. 9. Bar graphs of maximal stresses in legs (a) and platform mass (b) as functions of parameters D_{leg} and t_{leg} for platform leg spacing radius r_{leg} = 25 m.

CRITERION RESULTING FROM FATIGUE STRENGTH OF THE STRUCTURE

A basic criterion which should be taken into account when analysing the jack-up platform structure is fatigue strength. A simplified fatigue analysis was performed based on two-parameter Weibull distribution.

The main parameter describing the material effort is the largest stress range $\Delta\sigma_0$ recorded during n_0 cycles [29]

The range of normal stresses $\Delta\sigma_n$ was determined from the stress time-history shown in Fig. 10. The diagram presents stresses in platform legs, in the area close to leg fixing to the hull.

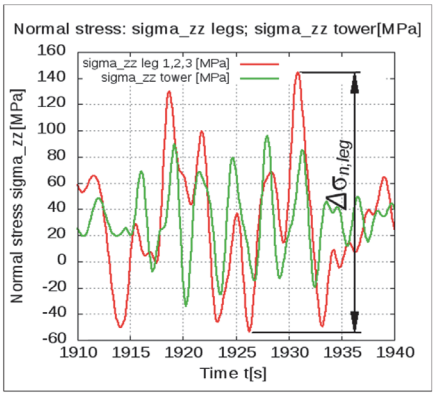

Fig. 10 Time-histories of stresses in legs $\sigma_{n,leg}$ (red), and in tower $\sigma_{n,tower}$ (green). Definition of maximal stress range $\Delta\sigma_{n,leg}$

The above definition of maximal stress range $\Delta\sigma_n$ was used to analyse the stress time-histories for the above matrix of cases. The results of this analysis are shown as bar graphs in Fig. 11.

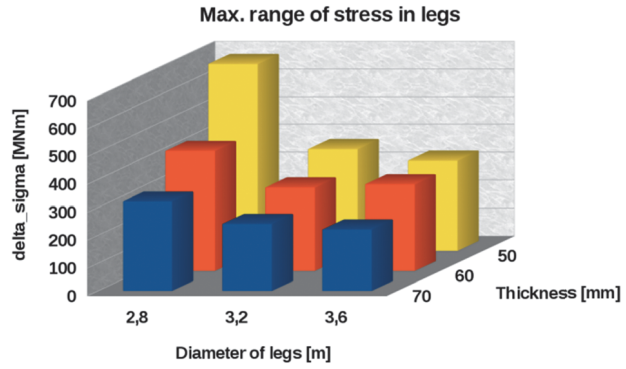

a)

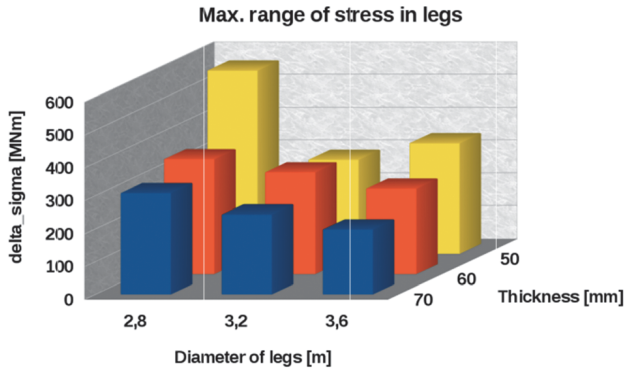

b)

Fig. 11 Maximal stress range $\Delta\sigma_{n,leg}$ for platform with leg spacing diameter: a) r_{leg} = 20 m, b) r_{leg} = 25 m

DETERMINING ACCEPTABLE STRESS RANGE

Before determining the acceptable stress range $\Delta\sigma_{all}$, the structure node (weld) should be selected which is most vulnerable with respect to fatigue strength.

Bearing in mind that the planned analysis is of preliminary nature and precise geometry in the areas of leg fixing to the hull and foots is not known yet, nodes were selected in leg (tube) parts situated beyond these areas.

Two nodes were selected, (see Fig. 12):

1. Node 1 was situated in the area of maximal bending moment appearance, i.e. in the leg part close to the hull and above water surface.

2. Node 2 was situated in the submerged part of the leg, in the area of maximal bending moment appearance, close to water surface.

An additional assumption was made that a transverse weld is situated in each of these areas, and the stress comes mainly from leg bending due to horizontal movements of the platform.

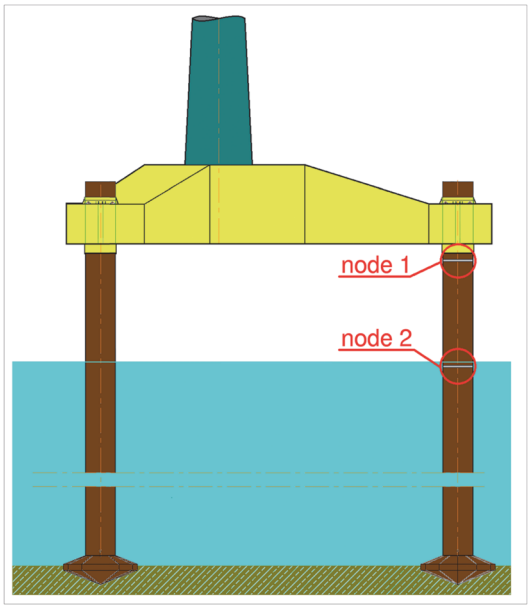

Fig. 12. Positions of structure nodes at which fatigue strength was analysed

FATIGUE STRENGTH ANALYSIS AT NODE 1

According to the relevant regulations [29] (Table A-9 and Table A-5), the C-type S-N curve was applied to the transverse weld shown in Fig. 12 as node 1. The assumed shape parameter of the adopted Weibull distribution was h=1.0.

The number of cycles expected during the platform lifetime, t_{life}=20 years, was determined as equal to 1.0·108, assuming that the duration of one cycle is T=6.3 s (as the average wave period).

For the C-type S-N curve and the shape coefficient h=1.0, the acceptable stress range for a structural element situated in air is $\Delta\sigma_{all}$ = 377.2 MPa ([29] Table 5-2).

The above stress range is given for the reference thickness, which is equal to t_{ref}=16 mm for pipe joints and 25 mm for remaining joints ([29], Par. 2.4.)

Correction of acceptable stresses due to wall thickness

When the plating/element thickness is greater than t_{ref}, the acceptable stress range is equal to ([29], Par. 5.2):

$$\Delta\sigma_{all,t} = \Delta\sigma_{all,tref}\left(\frac{t_{ref}}{t}\right)^k \quad \textbf{(22)}$$

The exponent k given in Table 2-3 [29] for pipe joints is k=0.25.

The acceptable stress ranges, calculated as a function of thickness t, are equal to:

$\Delta\sigma_{all,50mm}$ = 283.7 MPa; $\Delta\sigma_{all,60mm}$ = 271.1 MPa; $\Delta\sigma_{all,70mm}$ = 260.8 MPa

Design Fatigue Factor DFF

Design fatigue factors are used to decrease the likelihood of appearance of fatigue damage. The *DFF* value depends on the importance (function) of the structural element, as well as

on the accessibility (and frequency) of inspections of a given structure fragment, along with possible future repairs. [29]

If the consequences of structural damage are assessed as small and the structure meets the requirements of ALS [Accidental Limit States], then the following *DFF* values apply (depending on inspection accessibility) [30]:

Tab.5. Design fatigue factors, DFF, in relation to structure area [30]

DFF	*Structural element*
1	Internal structure, accessible and not welded directly to the submerged part.
1	External structure, accessible for regular inspection and repair in dry and clean conditions.
2	Internal structure, accessible and welded directly to the submerged part.
2	External structure not accessible for inspection and repair in dry and clean conditions.
3	Non-accessible areas, areas not planned to be accessible for inspection and repair during operation.

Although the platform leg parts situated above water surface are easily accessible for inspection, a pessimistic variant was assumed that no structure repairs are planned during 20 years of platform operation. Consequently, the assumed DFF value based on Table 5 is *DFF*=3.

After 20 years, a general overhaul of the structure (with possible repairs of elements) is planned to receive approval for its further operation.

The utilisation factor, read from [29], Table 5-8 for *DFF*=3 and t_{life}=20 years, is η=0.33. The considered node is in the air, above water surface.

The utilisation factor η=0.33 and the assumed Weibull distribution shape parameter *h*=1 were used for determining the acceptable stress reduction coefficient, C_r=0.748 ([29], Table 5-5)

The final reduced acceptable stress was calculated from formula:

$$\Delta\sigma_{all,t,\eta} = C_r \cdot \Delta\sigma_{all,t} \tag{23}$$

Hence:

$\Delta\sigma_{all,50mm,0.33}$ = 0.748·283.7 MPa = 212.2MPa
$\Delta\sigma_{all,60mm,0.33}$ = 0.748·271.1 MPa = 202.8 MPa
$\Delta\sigma_{all,70mm,0.33}$ = 0.748·260.8 MPa = 195.1 MPa

The nominal stress ranges obtained from the platform dynamics calculations are shown in Fig 11.

These ranges should be properly increased if the stress concentration resulting from connecting elements with different plating thickness takes place at the analysed node ([29], Par. 3.3). Moreover, the stress concentration increases when the connected leg segments are not coaxial and/or with deviations from roundness.

The stress concentration coefficient for the pipe joint of two elements with the same plating thickness is given by formula [29]:

$$SCF = 1 + \frac{3(\delta_m - \delta_0)}{t} e^{-\alpha} \tag{24}$$

where:

δ_m – maximal plating eccentricity, see Fig. 13.

δ_0 – characteristic eccentricity for S-N data for butt welds. For pipe joints δ_0=0.05t.

L – weld face width

$\alpha = \frac{0.91\,L}{\sqrt{Dt}}$, where D is the diameter of the connected elements (here $D=D_{leg}$)

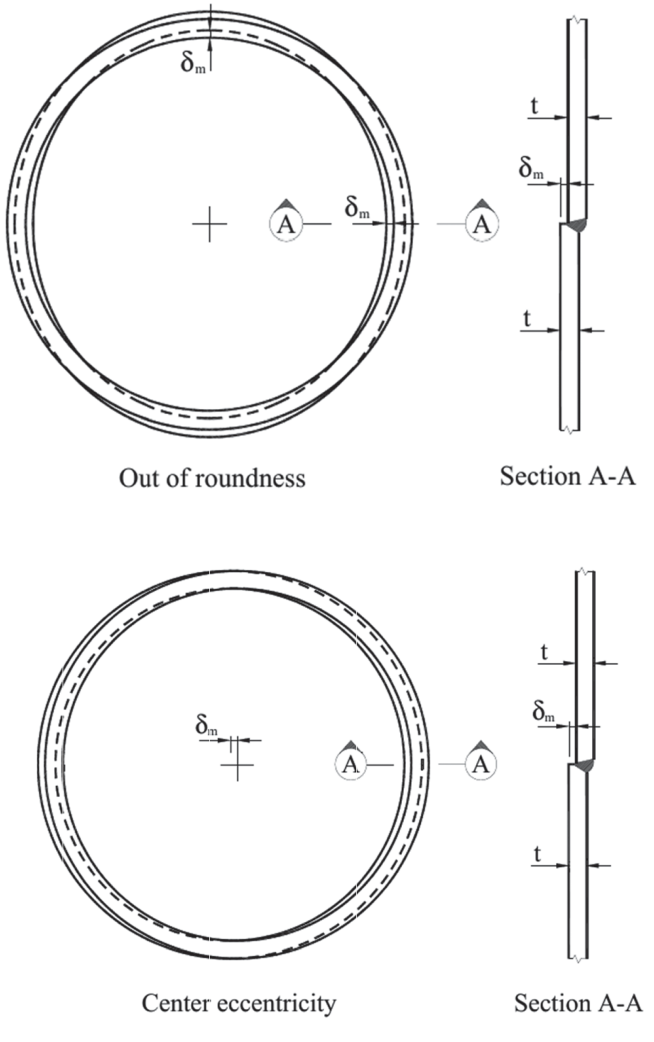

Fig. 13 Sketch presenting a procedure to determine geometric imperfection δ_m on butt weld of two pipe elements, according to DNV GL [29]

Here, an assumption was made that $\delta_m \le \delta_0$ (welds will be ground), hence *SCF*=1, which means that the stress concentration in the weld area does not exceed the value recorded in samples used to obtain the S-N data.

Table 6 collates the leg stress ranges $\Delta\sigma_o$ obtained from platform motion calculations. Additionally, the acceptable

stress ranges $\Delta\sigma_{all}$ corresponding to the thickness of the used plating are included.

Tab.6. Maximal stress ranges in jack-up platform legs as functions of leg plating thickness t_{leg} and leg diameter D_{leg}. Comparing with acceptable stress ranges for given thickness. Node 1.

	r_{leg} = 20 m			r_{leg} = 25 m			
	D_{leg}=2.8 m	D_{leg}=3.2 m	D_{leg}=3.6 m	D_{leg}=2.8 m	D_{leg}=3.2 m	D_{leg}=3.6 m	$\Delta\sigma_{all,t,0.33}$
t_{leg}=50 mm	672.4 MPa	365.9 MPa	324.5 MPa	558.5 MPa	286.4 MPa	336.9 MPa	212.2 MPa
t_{leg}=60 mm	431.3 MPa	299.7 MPa	310.7 MPa	349.9 MPa	309.7 MPa	259.9 MPa	202.8 MPa
t_{leg}=70 mm	321.5 MPa	242.3 MPa	222.0 MPa	308.2 MPa	243.9 MPa	198.6 MPa	195.1 MPa

Only the solution for the platform with leg spacing radius r_{leg} = 25 m, leg diameter D_{leg}=3.6 m, and plating thickness t=70 mm meets about all requirements concerning the fatigue stress of the structure, as $\Delta\sigma_o \approx \Delta\sigma_{all,70mm,0.33}$. A sketch of the area of acceptable solutions due to constraints resulting from impact and fatigue strength requirements is shown in Fig. 14. The diagram reveals that acceptable solutions should be searched within sets of parameters where the plating thickness tleg is larger than 70 mm and/or the leg diameter D_{leg} is larger than or equal to 3.6m. Acceptable solutions can also be found in the area with smaller plating thickness than t_{leg}=70 mm, but in those cases the leg diameter D_{leg} should be increased. Similarly, acceptable solutions can be found for leg diameters D_{leg} smaller than 3.6 m, but in those cases the increase of the plating thickness is very large and may reach values which would pose a challenge for present technologies.

Since the decisive factor in platform leg dimensioning is fatigue strength, a decision was made for the structure to be made mainly of normal-strength steel. Consequently, the assumed acceptable stress due to impact strength was 235 MPa.

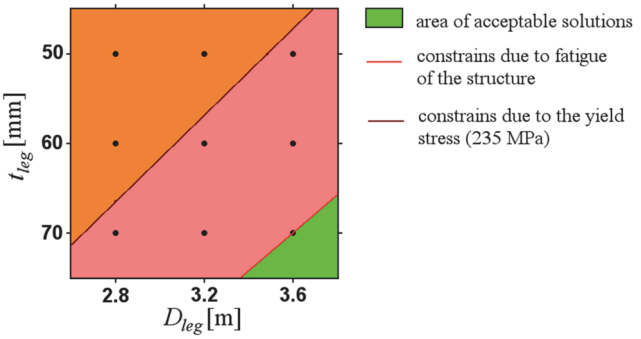

Fig. 14. Area of acceptable solutions with constraints for the structure with leg spacing radius rleg = 25 m. Node 1.

FATIGUE STRESS ANALYSIS AT NODE 2.

The basic differences between nodes 1 and 2 are:

- node 2 is situated lower (closer to the seabed), therefore the bending stresses will be smaller (as they are proportional to the distance from the seabed);
- node 2 is submerged (cathode protection is assumed), therefore the acceptable stresses for submerged nodes will be smaller.

The height of node 1 above seabed was H_{node1} = 52 m, while the height of node 2 is H_{node2} = 40 m. The plating thickness at node 2 is the same as that at node 1.

The stress range can be re-calculated for node 2 (for acceptable variant: t_{leg}=70 mm, D_{leg}=3.6 m, r_{leg}=25 m) as:

$$\Delta\sigma_{node2} = \Delta\sigma_{node1}\frac{H_{node2}}{H_{node1}} \tag{25}$$

The resulting value of the stress range for node 2 is $\Delta\sigma_{node2}$=152.8 MPa

The fatigue analysis for node 2 was performed for the same assumptions as for node 1. The only difference was that the structure fragment with node 2 is submerged in seawater and the cathode protection is applied.

The results of the fatigue analysis performed using a simplified method for node 2 are as follows:

The acceptable maximal stress range for components in seawater with cathode protection and for 1·108 cycles is $\Delta\sigma_{all}$=336.7 MPa, [29], Table 5-3.

The coefficient k given in Table 2-3 [29] for pipe joints is k=0.25. After substituting it to Equation 22, the obtained stress range is $\Delta\sigma_{\sigma all,70mm}$ = 232.8 MPa.

Node 2 is the area which is not accessible for inspection and not planned to be accessible for inspection and repair during structure's operation, therefore *DFF*=3. The utilisation factor read from [29], Table 5-8, for t_{life}=20 years is η=0.33.

The considered node is submerged in seawater and has cathode protection. Therefore, the acceptable stress reduction coefficient is C_r=0.785 ([29], Table 5-7).

The final value of the acceptable stress range for node 2 is: $\Delta\sigma_{all,70mm,0.33}$ = 0.785·232.8 MPa = 182.7 MPa.

Since the stress concentration coefficient for this weld is *SCF*=1, the stress range at node 2 meets the condition: $\Delta\sigma_{node2} \leq \Delta\sigma_{all,70mm,0.33}$

SUMMARY, CONCLUSIONS AND COMMENTS

Within the framework of the presented research, two jack-up platform concepts differing by leg spacing radius and hull dimensions were designed with the intention to be used as a supporting structure for a 6-MW offshore wind turbine.

For each concept, the parametric analysis was performed to determine optimal dimensions of platform legs: diameter D_{leg} and plating thickness t_{leg}. The platform motion was calculated for conditions characteristic for most violent storm in recent 50 years on the South Baltic area, for the platform parameters given in Table 1.

The obtained results, having the form of amplitudes of selected physical quantities, are shown in comprehensive charts in Fig. 6 and 7. Based on the critical stress values (corresponding to the yield stress), the area was defined in which the impact strength conditions are satisfied (Fig. 14).

The fatigue strength analysis was performed for two selected critical leg nodes. Its results were used for defining the acceptable area with respect to structure's fatigue (Fig. 14). Geometric parameters were determined which meet the adopted criteria, Table 6.

The decisive criterion turned out to be the fatigue strength criterion, while the yield point criterion appeared to be an inactive constraint.

In practice, the only solution which meets the fatigue strength criterion (along with the impact strength criterion) is the solution with the following set of parameters:
r_{leg}=25.0 m, D_{leg}=3.6m, t_{leg}=70mm.

Extrapolating the obtained results, we can conclude that the above criteria will also be met by platforms with leg diameter D_{leg} greater than 3.6m, and platforms with plating thickness t_{leg} greater than 70mm. However, the mass of legs in those solutions will be larger. Decreasing the leg diameter is also possible, but it would require proper increase in plating thickness. Similarly, reducing the leg plating thickness is possible, at simultaneous increase of leg diameter (Fig. 14).

It is noteworthy that the presented method is applicable for preliminary selection of basic dimensions of the platform, especially leg dimensions. The analyses described in the article were simplified, as they referred to the parametric design stage, when no complete geometric model of the structure is available. Major simplifications assumed in the analyses were constant values of wind speed and turbine thrust coefficient C_T. These simplifications originated from the fact that for the assumed conditions, the dominating loads were hydrodynamic forces generated by waves.

Further research and design steps will include analysing the operation of the turbine-tower-supporting structure system in various weather conditions. It will also take into account loads generated by wind (to meet the requirements formulated in the relevant Standard [31]).

ACKNOWLEDGEENT

This research was supported by the Polish National Centre for Research and Development (NCBR) under the project "WIND-TU-PLA" ERA-NET MARTEC II (Agreement No. MARTECII/1/2014)

REFERENCES

1. GWEC. (2018). Global Wind Statistics 2017. Global Wind Energy Council, 14 February 2018.

2. http://www.polenergia.pl/pol/pl/strona/farmy-morskie (12/12/2018)

3. https://www.equinor.com/en/what-we-do/hywind-where-the-wind-takes-us.html (12/12/2018)

4. Fukushima Floating Offshore Wind Farm Demonstration Project (Fukushima FORWARD). Source: http://www.fukushima-forward.jp/pdf/pamphlet3.pdf (13/12/2018)

5. Fulton G.R., Malcolm D.J., Elwany H., Stewart W., Moroz E., Dempster H.: Semi-Submersible Platform and Anchor Foundation Systems for Wind Turbine Support. National Renewable Energy Laboratory (U.S.), Subcontract Report NREL/SR-500-40282, December 2007

6. Bachynski E.E., Moan T. (2012). Design considerations for tension leg platform wind turbines. Marine Structures 29 (2012) 89–114.

7. Żywicki J., Dymarski P., Ciba E., Dymarski C. (2017). Design of Structure of Tension Leg Platform for 6 MW Offshore Wind Turbine Based on Fem Analysis. Polish Maritime Research 24(s1), 230-241. https://doi.org/10.1515/pomr-2017-0043

8. Dymarski C., Dymarski P., Żywicki J. (2017). Technology Concept of TLP Platform Towing and Installation in Waters with Depth of 60 m. Polish Maritime Research 24(s1), 59-66. https://doi.org/10.1515/pomr-2017-0022

9. Karimirad M., Moan T. (2012). Feasibility of the Application of a Spar-type Wind Turbine at a Moderate Water Depth. DeepWind, 19-20 January 2012, Trondheim, Norway. Energy Procedia 24(2012) 340-350

10. Duan F., Hu Z., Niedzwecki J.M. (2016). Model test investigation of a spar floating wind turbine. Marine Structures 49 (2016) 76-96

11. Dymarski P. Ciba E. (2017). Design of a cell-spar platform for a 6 MW wind turbine. Parametric analysis of the mooring system. Twenty First International Conference on Hydrodynamics in Ship Design and Operation - HYDRONAV, Gdańsk, 28-29 June 2017

12. Yeter B., Garbatov Y., Soares C.G. (2014). Fatigue damage analysis of a fixed offshore wind turbine supporting structure. Developments in Maritime Transportation and Exploitation of Sea Resources, Taylor & Francis Group, London

13. Velarde J., Bachynski E.E. (2017). Design and fatigue analysis of monopile foundations to support the DTU 10 MW offshore wind turbine. 14th Deep Sea Offshore Wind R&D Conference, EERA DeepWind'2017, 18-20 January 2017, Trondheim, Norway. Energy Procedia 137 (2017) 3–13

14. Bogdaniuk M. (2017). Estimation of the fatigue life of the hull of TLP [in Polish]. Technical Report. Polish Register

of Shipping, Gdańsk 2017

15. Rozmarynowski B., Mikulski T. (2018). Selected problems of sensitivity and reliability of a jack-up platform. Polish Maritime Research 25(1(97)), 77-84. https://doi.org/10.2478/pomr-2018-0009

16. Dymarski C., Dymarski P., Żywicki J. (2015). DESIGN AND STRENGTH CALCULATIONS OF THE TRIPOD SUPPORT STRUCTURE FOR OFFSHORE POWER PLANT. Polish Maritime Research 22(1(85)), 36-46. https://doi.org/10.1515/pomr-2015-0006

17. Kahsin M., Łuczak M. (2015). Numerical Model Quality Assessment of Offshore Wind Turbine Supporting Structure Based on Experimental Data. Structural Health Monitoring 2015: System Reliability for Verification and Implementation: Proceedings of the 10th International Workshop on Structural Health Monitoring. Vol. 1/ ed. Fu-Kuo Chang, Fotis Kopsaftopoulos 439 North Duke Street · Lancaster, PA 17602-4967, U.S.A. : DEStech Publications, Inc., 2015, 2817-2824

18. Wilson J.F.: Dynamics of Offshore Structures (2nd Edition). John Wiley & Sons, Inc., Hoboken, New Jersey, 2003

19. Chandrasekaran S.: Dynamic Analysis and Design of Offshore Structures (Ocean Engineering & Oceanography). Springer, New Delhi, 2015

20. Sarpkaya T. Wave Forces on Offshore Structures. Cambridge University Press, New York, 2010

21. Offshore Standards DNV-OS-J103 (2013). Design of Floating Wind Turbine Structures. Det Norske Veritas, June 2013

22. Niezgodziński M.E., Niezgodziński T.: Strength formulas, diagrams, and tables [in Polish]. WNT, Warszawa 2013.

23. Dymarski P., Ciba E., Marcinkowski T. (2016). Effective method for determining environmental loads on supporting structures for offshore wind turbines. Polish Maritime Research 23(1(89)), 52-60. https://doi.org/10.1515/pomr-2016-0008

24. Recommended Practice DNV-RP-C205 (2010). Environmental Conditions and Environmental Loads. Det Norske Veritas, October 2010

25. Sarpkaya T. (1986). In-line and transverse forces on smooth and rough cylinders in oscillatory flow at high Reynolds numbers, Monterey, California. Naval Postgraduate School

26. Product Portfolio Overview. The Senvion 6.XM series.

27. Jonkman J., Butterfield S., Musial W., Scott G. (2009). Definition of a 5-MW Reference Wind Turbine for Offshore System Development. National Renewable Energy Laboratory, Technical Report NREL/TP-500-38060 February 2009

28. Kooijman H.J.T., Lindenburg C., Winkelaar D., van der Hooft E.L. (2003). DOWEC 6 MW PRE-DESIGN. Aero-elastic modelling of the DOWEC 6 MW pre-design in PHATAS. Report DOWEC-F1W2-HJK-01-046/9 (public version). September 2003

29. Recommended Practice DNVGL-RP-C203 (2016). Fatigue design of offshore steel structures. DNV GL, April 2016

30. Offshore Standards DNVGL-OS-C101 (2016). Design of offshore steel structures, general - LRFD method. April 2016

31. EUROPEAN STANDARD IEC 61400-3 (2009). Wind turbines - Part 3: Design requirements for offshore wind turbines (IEC 61400-3:2009)

CONTACT WITH THE AUTHOR

Paweł Dymarski
e-mail: pawdymar@pg.edu.pl

Gdańsk University of Technology
Faculty of Ocean Engineering and Ship Technology
Narutowicza 11/12
80-233 Gdansk
Poland